

## Influence of sputtering gas pressure on the $\text{LiCoO}_2$ thin film cathode post-annealed at 400 °C

Ho Young Park, Sang Cheol Nam<sup>†</sup>, Young Chang Lim, Kyu Gil Choi, Ki Chang Lee, Gi Back Park, Heesook Park Kim\* and Sung Baek Cho\*\*

Microcell Center, Nuricell Inc., #503, Sinnae Technotown, 485 Sangbong-dong, Joongrang-gu, Seoul 131-863, Korea

\*College of General Education, Kookmin University, Seoul 136-702, Korea

\*\*Advanced Technology Research Center, Agency for Defense Development, Yuseong P.O. Box 35, Daejeon 305-600, Korea

(Received 26 October 2005 • accepted 17 March 2006)

**Abstract**— $\text{LiCoO}_2$  thin film cathodes were prepared by RF magnetron sputtering and post-annealing. The surface morphological change of the  $\text{LiCoO}_2$  thin film was *in-situ* measured by hot stage SEM with increasing temperature. The effects of sputtering gas pressure and post-annealing at low temperature (400 °C) were investigated by XRD, AFM, ICP-AES and RBS. The electrochemical characteristics of  $\text{LiCoO}_2$  thin films were changed with variation of sputtering gas pressure. A difference of micro-structural evolution after post-annealing was observed, which related to the thin film properties. The electrochemical analysis revealed that the optimal sputtering gas pressure with the low temperature annealing step increases cell capacity and rate capability.

Key words: Lithium Cobalt Oxide, Thin Film Battery, RF Sputtering, Low Temperature Annealing

### INTRODUCTION

There is a growing interest in thin film batteries in view of multiple applications in microelectronics [Bates et al., 2000]. They show considerably good thermal stability, low self discharge and high rate discharge capability, because all battery components consist of solid thin films [Bates et al., 1993]. The lithium intercalation materials with layered rock salt structure have been shown to be well suited for lithium batteries as cathode active materials. Recently, lithium cobalt oxide ( $\text{LiCoO}_2$ ) has received great interest from many researchers due to a high operating potential of ~4 V and reversible capacity of ~137 mAh g<sup>-1</sup>. The  $\text{LiCoO}_2$  powders used for conventional lithium ion battery have been known to exhibit different characteristics in their electrode behavior with the synthesis methods [Rossen et al., 1993; Yan et al., 1998; Bhat et al., 2000]. In the case of thin film batteries, since thin film batteries using  $\text{LiCoO}_2$  cathode have been developed in Oak Ridge National Laboratory by RF sputtering method, many research groups have tried to fabricate the thin film cathode [Wang et al., 1993; Antaya et al., 1993; Lee et al., 1996, 1999; Striebel et al., 1996; Song et al., 2000; Whitacre et al., 2001; Bates et al., 2000; Fragnaud et al., 1996; Polo da Fonseca et al., 1999; Bouwman et al., 2001]. Generally, microstructural evolution, composition, morphology and electrochemical properties of thin films are strongly dependent on deposition process parameters. However, it is noted that the sputtering process parameters of  $\text{LiCoO}_2$  thin film deposition has not been thoroughly investigated.

$\text{LiCoO}_2$  thin films deposited by RF magnetron sputtering at room temperature have an amorphous structure (no X-ray diffraction peak); they have less density than the corresponding crystalline materials. Therefore, it is known that the high temperature annealing at ca. 700 °C is needed to obtain the crystalline structure for reversible

intercalation/deintercalation of lithium ions. However, the post-annealing process at high temperature is likely to damage substrate including under-layers, e.g., metallic current collectors or electronic components connected to the thin film batteries [Whitacre et al., 2001; Benqlilou-Moudden et al., 1998]; the post-annealing step is not compatible with integrated silicone-based devices, flexible polymer or metallic substrate. There was nevertheless little investigation on  $\text{LiCoO}_2$  thin films by low temperature process.

In this study, physical and electrochemical properties of  $\text{LiCoO}_2$  thin films by RF magnetron sputtering were investigated in accordance with sputtering gas pressure change as the process parameter. Further, we described the characteristics of the  $\text{LiCoO}_2$  thin films obtained by low annealing temperature process without exceeding 400 °C, which were applicable to the cathode materials for thin film battery.

### EXPERIMENTAL

$\text{LiCoO}_2$  thin film cathodes were prepared by RF magnetron sputtering onto current collector, which was subsequently deposited by  $\text{Pt}(250 \text{ nm})/\text{TiO}_2(12 \text{ nm})/\text{Ti}(30 \text{ nm})$  on Si wafer. Before deposition, pre-sputtering was conducted under pure argon atmosphere for 20 min to remove contaminant of target surface. The substrate was rotated at 10 rpm in order to improve the film homogeneity. The sputtering target was fabricated by lithium cobalt oxide powder (Seimi). Powder was ball-milled for 24 h after calcination at 500 °C. The pressed target at 100 kgf cm<sup>-2</sup> in addition of 2 wt% PVA binder was sintered at 1,000 °C for 3 h. The distance between target and substrate was 13 cm and the applied RF power was constant to 200 W using 4 inch target. The base pressure was  $5 \times 10^{-6}$  torr and total working pressure was maintained at 3, 8, 13 and 18 mtorr, respectively, with the  $\text{O}_2/\text{Ar}$  gas ratio of 2/8. Film thickness was determined by alpha step (P1, Tencor) and fixed to 200 nm. Although, substrate was not heated by additional heating elements, the temperature was

\*To whom correspondence should be addressed.

E-mail: scnam@nuricell.com

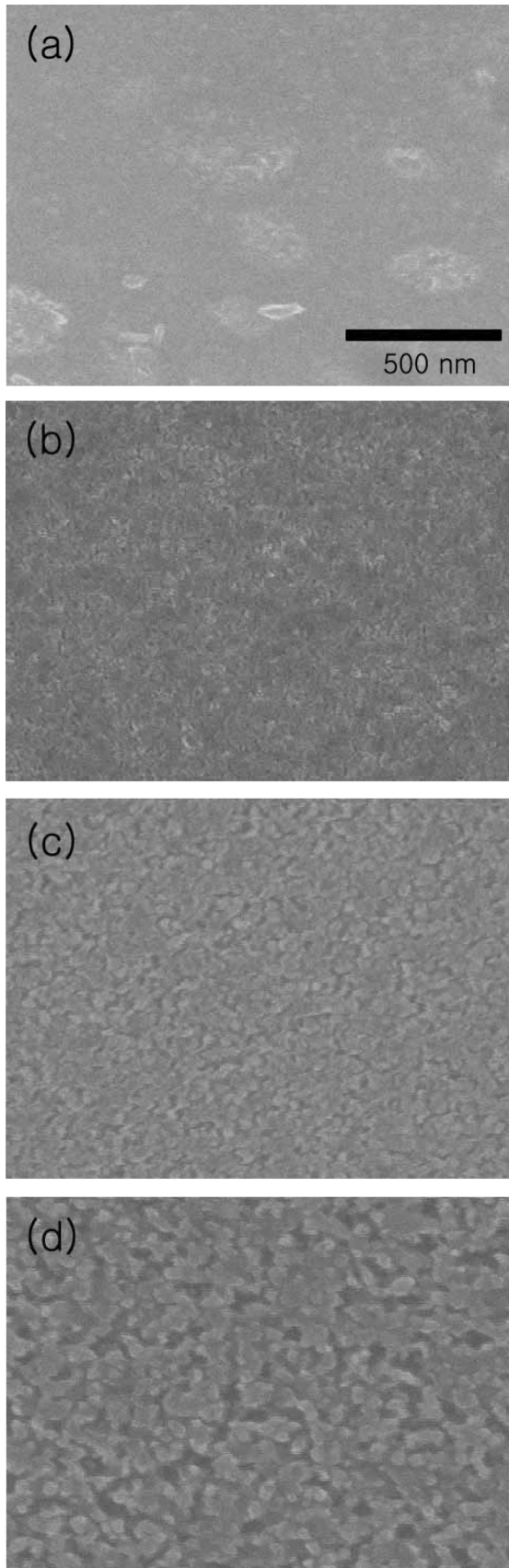


Fig. 1. Scanning electron microscope images of  $\text{LiCoO}_2$  thin film by *in-situ* annealing at (a) 300 °C, (b) 400 °C, (c) 500 °C, and (d) 600 °C.

increased to about 100°C during deposition, which was measured by thermocouple contacted to substrate. The film surface morphological change was measured by *in-situ* hot stage scanning electron microscopy (SEM, Philips EX-30) from 300 °C to 700 °C. Post-annealing was conducted at 400 °C for 5 h under atmospheric condition. Li/Co and Co/O ratios were analyzed by inductively coupled plasma-atomic emission spectroscopy (ICP-AES, Thermojarrell ASH) and rutherford backscattering spectroscopy (RBS, NEC 6SDH-2), respectively. Surface roughness and structure were measured by atomic force microscopy (AFM, PSI-CP) and x-ray diffraction analysis (XRD, Rigaku). Cells were assembled with lithium foil (FMC) as counter and reference electrodes and 1 M  $\text{LiPF}_6$  in EC : DMC (1 : 1, Merck) as the electrolytic solution and polyethylene-based separator (Ube) was used. Constant current galvanostatic charge/discharge tests and cyclic voltammetry were performed by a battery cycler system (WBCS 3000).

## RESULTS AND DISCUSSION

Fig. 1 shows the surface morphological change of the  $\text{LiCoO}_2$  thin film deposited at 18 mtorr using *in-situ* hot stage SEM with increasing temperature. The ramping up speed was 4 °C min<sup>-1</sup>. Tiny

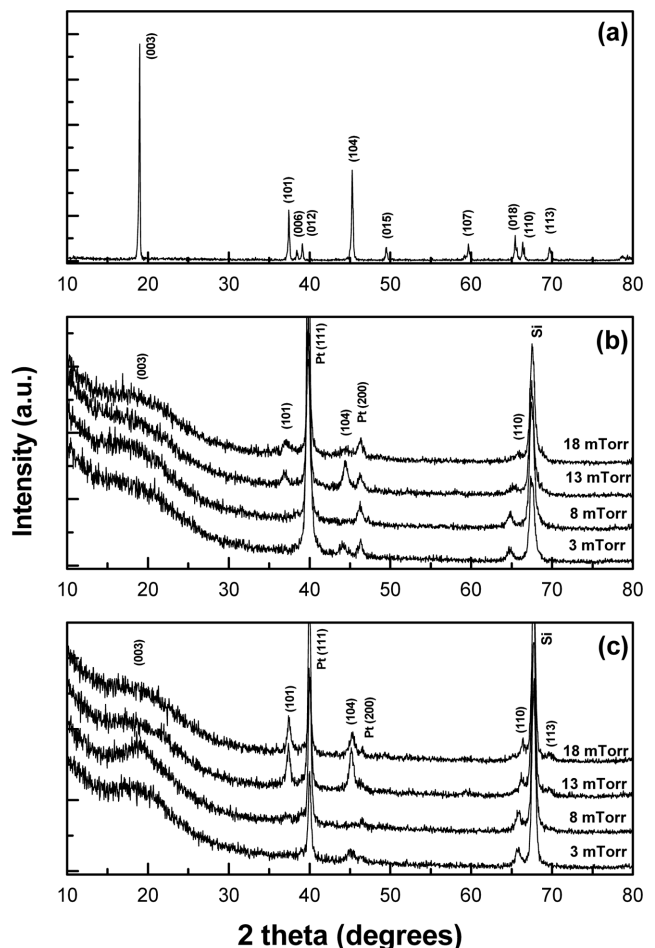
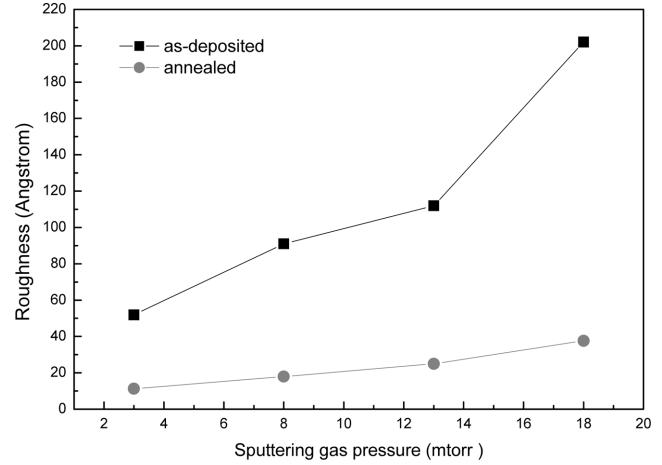


Fig. 2. X-ray diffraction patterns of the (a)  $\text{LiCoO}_2$  target, (b) as-deposited, and (c) annealed at 400 °C  $\text{LiCoO}_2$  thin films with sputtering gas pressures.

crystallites were created and grown through coalescence from 400 °C. Such phenomena were similar to other sputtering gas conditions. The determined post annealing condition at 400 °C is based on this result.

Fig. 2 shows the XRD patterns of (a) sputtering target, (b) as-deposited, and (c) annealed at 400 °C for 5 h. The typical hexagonal R-3m LiCoO<sub>2</sub> structure was shown in sputtering target. While the as-deposited LiCoO<sub>2</sub> thin films have some crystal peaks at 13 mtorr and 18 mtorr, preferred orientations of (101) and (104) grains were well developed after post-annealing process (Fig. 2(b) and (c)). However, XRD patterns at 3 mtorr and 8 mtorr did not exhibit a remarkable difference between as-deposited and post-annealed samples.

The three-dimensional AFM images of the as-deposited and post-annealed LiCoO<sub>2</sub> thin film which area of 1 μm × 1 μm are shown in Fig. 3, and the z-axis was fixed to same scale. While the clusters were formed at as-deposited films, smooth surfaces were shown after post-annealing process. It could be thought that the surface area was decreased to maintain low surface energy, because the contribution of surface free energy is dominant than volume free energy in thin films when re-crystallization occurs during annealing process. Such behaviors were cleared by roughness change. As shown



**Fig. 4. Surface roughness of LiCoO<sub>2</sub> thin film as a function of sputtering gas pressures.**

in Fig. 4, the average root-mean-square ( $R_{rms}$ ) of the surface roughness was increased as the sputtering gas pressure increase with or without annealing. It could be supposed that the local clusters were

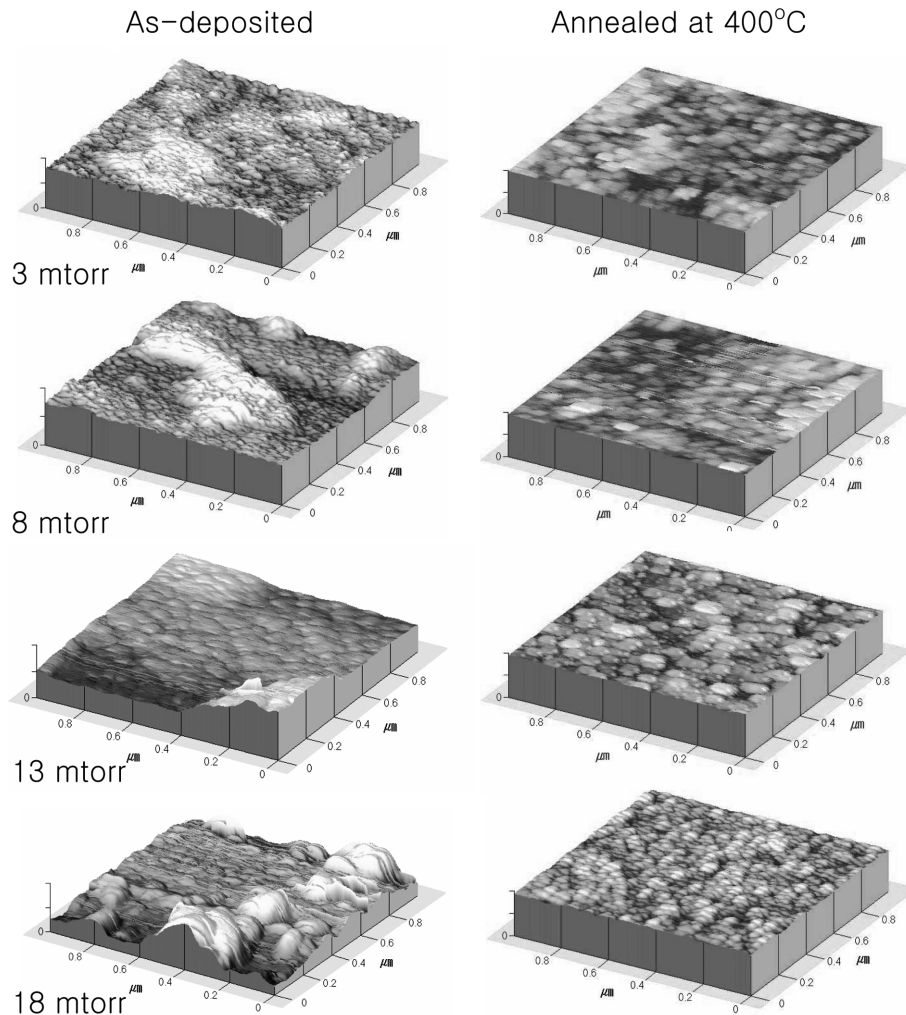


**Fig. 3. Atomic force microscope images of the LiCoO<sub>2</sub> thin film with various sputtering gas pressures.**

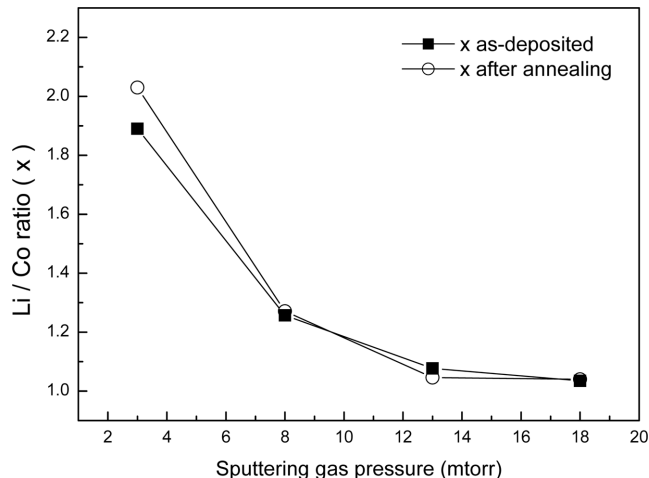


Fig. 5. Li/Co molar ratio (x) with the change of sputtering gas pressures by ICP-AES.

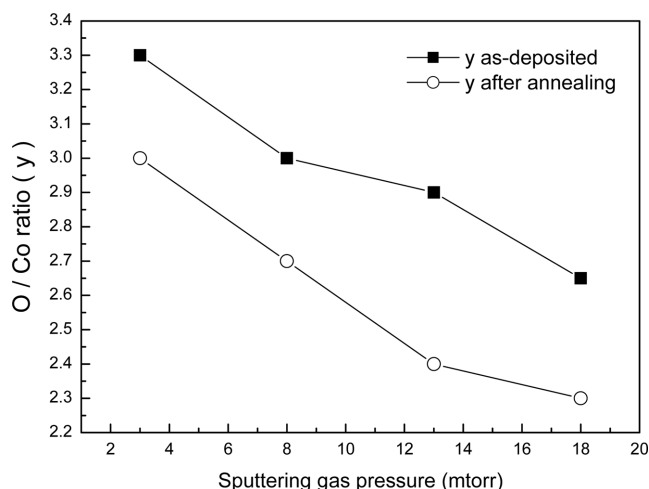


Fig. 6. O/Co molar ratio (y) with the change of sputtering gas pressures by RBS.

formed due to retarding nucleation reaction as a result of high existence probability of the sputtering gas onto the substrate surface as the sputtering gas pressure increased, which induces a crystallinity difference in the growing film.

The Li/Co and O/Co molar ratios were analyzed by ICP-AES and RBS, respectively. As shown in Fig. 5, the amount of lithium was decreased as the sputtering gas pressure increased. Also, the oxygen molar ratio to cobalt shows similar behavior (Fig. 6). With combining lithium and oxygen molar ratios into cobalt based  $\text{Li}_x\text{CoO}_y$  composition, total composition of the cathode thin film approached to theoretical stoichiometry of the  $\text{LiCoO}_2$  with increasing the sputtering gas pressure. It can be described that a light element such as lithium is easy to be scattered by collision of sputtering gas atoms and re-sputtered from the substrate, resulting in low lithium contents at high sputtering gas pressures. Moreover, it was proven to have a close relationship between oxygen and lithium contents. The Li and O contents were rich at low sputtering gas pressures, and showed discrepancy of typical  $\text{LiCoO}_2$  composition. Thus, it could create a second phase after the post-annealing process. While the

lithium content did not show large variation, oxygen content was decreased after post-annealing. Generally, as-deposited  $\text{LiCoO}_2$  thin film has nano-crystallites arranged randomly with short range order. In this case, prevalent inter-grain boundaries exist in thin film. It is estimated that excess oxygen is due to existence of corner-shared oxygen octahedrons in this boundary region as well as edge-shared octahedrons for  $\text{LiCoO}_2$  crystalline phase. So, it could be thought that the volume ratio of the boundary region after post annealing was decreased as a result of the grain growth, resulting in gradual decrease of excess oxygen content with long range ordered grains.

From aforementioned AFM, ICP-AES and RBS data, it is thought that these kinds of crystallinity difference depend on the compositions and micro-structures of the as-deposited  $\text{LiCoO}_2$  thin film, and it is preferable to deposit the  $\text{LiCoO}_2$  thin film at higher sputtering gas pressures to increase the crystallinity in the condition of low annealing temperature. This also means that the crystallinity deposited at relatively high sputtering gas pressure could be higher than that of the low pressures. These results are well consistent with XRD patterns in Fig. 2.

Fig. 7 shows the charge/discharge characteristics of the as-deposited and post annealed  $\text{LiCoO}_2$  cathode thin film with various sputtering gas pressures when the constant current of 20  $\mu\text{A}$  was applied. The charge/discharge capacities with post-annealing were higher than the as-deposited thin films at all working pressures. While the as-deposited  $\text{LiCoO}_2$  thin film cathode showed continuous linear potential drop, post-annealed sample revealed the similar behavior

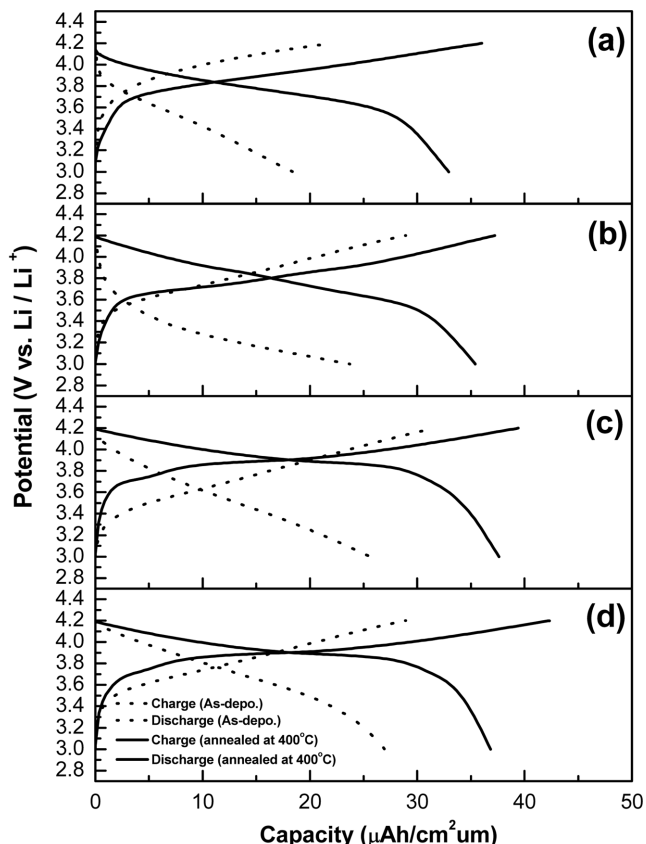


Fig. 7. Charge/discharge performances of  $\text{LiCoO}_2$  thin film with sputtering gas pressure of (a) 3 mTorr; (b) 8 mTorr; (c) 13 mTorr; and (d) 18 mTorr.

to the typical  $\text{LiCoO}_2$  cathode. The  $\text{LiCoO}_2$  thin films deposited at 13 mtorr and 18 mtorr have the plateau region and the capacity was larger than that of the 3 mtorr and 8 mtorr. It was found that the plateaus could be shown at 3.7 V (vs.  $\text{Li}/\text{Li}^+$ ), 3.9 V (vs.  $\text{Li}/\text{Li}^+$ ) during charging and shown at 3.8 V (vs.  $\text{Li}/\text{Li}^+$ ) and 3.6 V (vs.  $\text{Li}/\text{Li}^+$ ) during discharging process in post annealed  $\text{LiCoO}_2$  thin film deposited at 8 mtorr, while it was difficult to classify plateaus at 3 mtorr. The redox potential at 3.9 V (vs.  $\text{Li}/\text{Li}^+$ ) and 3.8 V (vs.  $\text{Li}/\text{Li}^+$ ) is caused by inter/deintercalation reaction of the typical HT- $\text{LiCoO}_2$  phase; however it is known that the redox potential appears at 3.7 V (vs.  $\text{Li}/\text{Li}^+$ ) and 3.6 V (vs.  $\text{Li}/\text{Li}^+$ ) in LT- $\text{LiCoO}_2$  phase [Rossen et al., 1993]. Although HT-characteristics were more dominant with increasing sputtering pressure, LT-behaviors were also observed in the samples prepared at 13 mtorr and 18 mtorr, which indicates that complete hexagonal structure could not be formed at relatively low annealing temperature. Thus, resulting thin films show a relatively low capacity (ca. 38  $\mu\text{Ah}/\text{cm}^2\cdot\mu\text{m}$ ) compared to the theoretical value of  $\text{LiCoO}_2$  cathode thin film (ca. 69  $\mu\text{Ah}/\text{cm}^2\cdot\mu\text{m}$ ).

Fig. 8 shows the cyclic voltammograms of the as-deposited and annealed  $\text{LiCoO}_2$  thin film with various sputtering gas pressures. Post annealed  $\text{LiCoO}_2$  thin films showed good reversibility in all gas pressure conditions. As expected, redox peaks were developed

as the sputtering gas pressure increased. Especially, oxidation peaks near 3.7 V (vs.  $\text{Li}/\text{Li}^+$ ) and 3.9 V (vs.  $\text{Li}/\text{Li}^+$ ) were separated with the same height at 8 mtorr, corresponding to reduction peaks near 3.7 V (vs.  $\text{Li}/\text{Li}^+$ ) and 3.6 V (vs.  $\text{Li}/\text{Li}^+$ ), and it is thought that it is due to the HT- $\text{LiCoO}_2$  and LT- $\text{LiCoO}_2$  mixed phase. In the case of high working pressures, while a peak corresponding to HT- $\text{LiCoO}_2$  was developed, peaks corresponding to LT- $\text{LiCoO}_2$  phase were linearly decreased. Although, these trends could not be clarified in XRD results in Fig. 2, because hexagonal R-3m symmetry of HT- $\text{LiCoO}_2$  and spinel Fd3m symmetry of LT- $\text{LiCoO}_2$  have a similar pattern, it is presumed that the LT- $\text{LiCoO}_2$  could exist due to no peak separation of (108) and (110) planes near  $2\Theta=66^\circ$  [Rossen et al., 1993; Antaya et al., 1994]. However, it could be clearly defined that the LT- $\text{LiCoO}_2$  phase exists through electrochemical analysis. It could be described that the LT- $\text{LiCoO}_2$  phase of Fd3m was partially formed by disordering of Li and Co cation during annealing process, caused by difference of  $\text{LiCoO}_2$  stoichiometrical composition.

The rate capabilities of the  $\text{LiCoO}_2$  thin film annealed at 400 °C for 5 h are shown in Fig. 9. As the sputtering gas pressure increased, ohmic drop was reduced. When the discharge current of 0.3 mA was applied, discharge capacity of more than 80% of the normalized capacity could be obtained for sample deposited at 18 mtorr. These

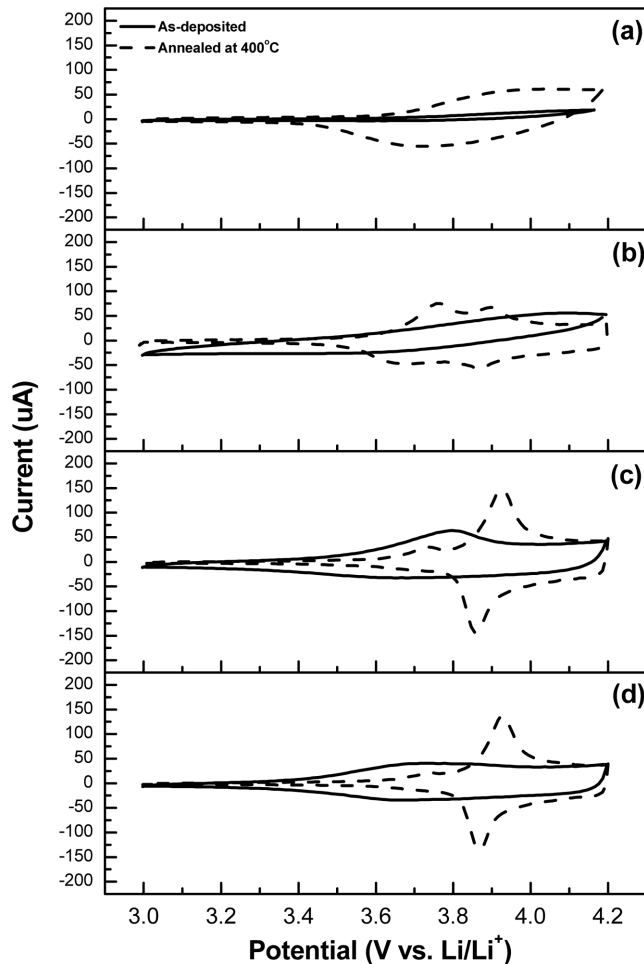


Fig. 8. Cyclic voltammograms of  $\text{LiCoO}_2$  thin films with sputtering gas pressure of (a) 3 mTorr; (b) 8 mTorr; (c) 13 mTorr; and (d) 18 mTorr.

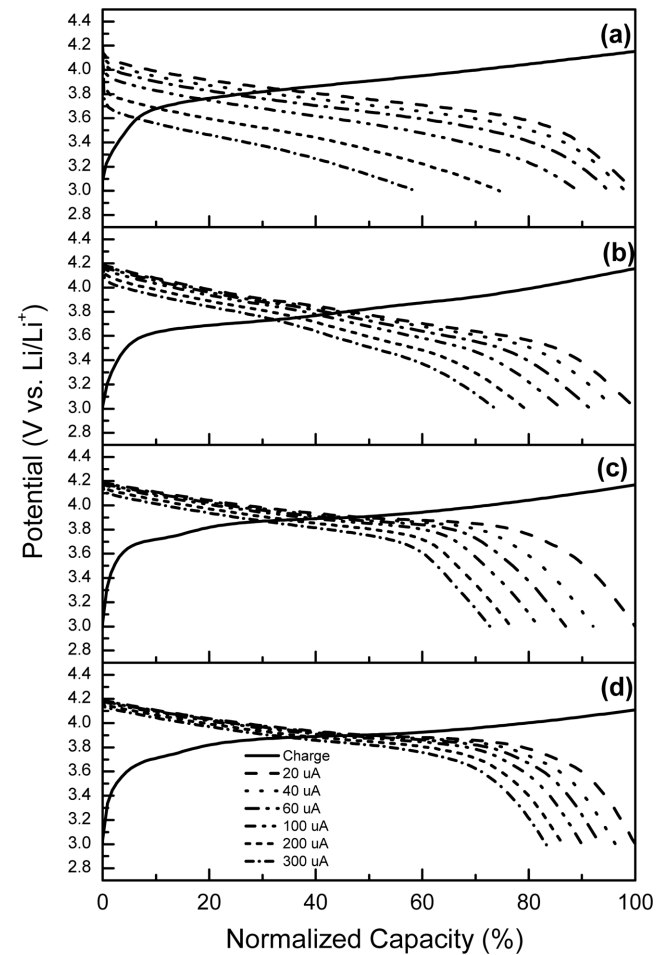
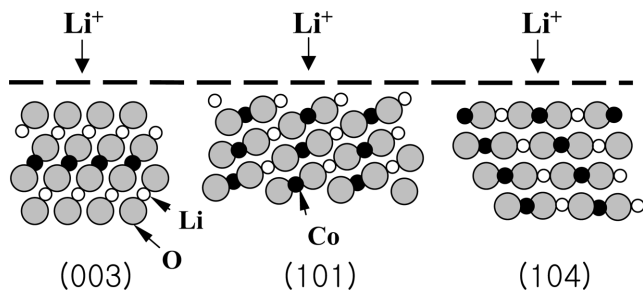


Fig. 9. Rate capabilities of  $\text{LiCoO}_2$  thin films with sputtering gas pressure of (a) 3 mTorr; (b) 8 mTorr; (c) 13 mTorr; and (d) 18 mTorr.



**Fig. 10. Schematic diagram of the preferred orientation of  $\text{LiCoO}_2$  grains.**

kinds of good high rate discharge capacities are due to the easy Li diffusion path and low contact resistance for uniform interface of the thin films.

Fig. 10 shows a schematic diagram of the preferred orientation of the  $\text{LiCoO}_2$  grains [Bates et al., 2000]. The (101) and (104) texture of the  $\text{LiCoO}_2$  thin film is useful for easy Li intercalation, while the closed packed (003) plane does not support an easy path. This means that preferred oriented (101) and (104) texture after post annealing contribute to the high rate discharge performances.

## CONCLUSIONS

As-deposited  $\text{LiCoO}_2$  thin film cathode at various sputtering gas pressures showed micro-structural change and revealed different crystallinity after post-annealing at relatively low temperature (400 °C). The amount of Li and O was decreased as the sputtering gas pressure increased, and total composition of thin film approached to theoretical stoichiometry of the  $\text{LiCoO}_2$  with increasing the sputtering gas pressures. While the LT- and HT- $\text{LiCoO}_2$  mixed phase was formed at low sputtering gas pressures, it was changed to dominant HT- $\text{LiCoO}_2$  phase as the sputtering gas pressure increased, resulting in development of redox peaks. The  $\text{LiCoO}_2$  thin films deposited at high sputtering gas pressures showed good electrochemical reversibility, including rate capabilities and charge/discharge performances without thermally induced stress.

## ACKNOWLEDGMENTS

This work is supported by dual-use technology program of MND, Korea, and the Korea Basic Science Institute (Seoul) is acknowledged for the XRD data.

## REFERENCES

Antaya, M., Cearns, K., Preston, J. S., Reimers, J. N. and Dahn, J. R., "In situ growth of layered, spinel, and rock-salt  $\text{LiCoO}_2$  by laser ablation deposition," *J. Appl. Phys.*, **76**, 2799 (1994).

Antaya, M., Dahn, J. R., Preston, J. S., Rossen, E. and Reimers, J. N., "Preparation and characterization of  $\text{LiCoO}_2$  thin films by laser ablation deposition," *J. Electrochem. Soc.*, **140**, 575 (1993).

Bates, J. B., Dudney, N. J., Neudecker, B., Ueda, A. and Evans, C. D., "Thin-film lithium and lithium ion batteries," *Solid State Ionics*, **135**, 33 (2000).

Bates, J. B., Gruzalski, G. R., Dudney, N. J., Luck, C. F., Yu, X.-H. and Jones, S. D., "Rechargeable thin-film lithium microbatteries," *Solid State Technol.*, **36**, 59 (1993).

Benqlilou-Moudden, H., Blondiaux, G., Vinatier, P. and Levasseur, A., "Amorphous lithium cobalt and nickel oxides thin films: preparation and characterization by RBS and PIGE," *Thin Solid Films*, **333**, 16 (1998).

Bhat, M. H., Chakravarthy, B. P., Ramakrishnan, P. A., Levasseur, A. and Rao, K. J., "Microwave synthesis of electrode materials for lithium batteries," *Bull. Mater. Sci.*, **23**, 461 (2000).

Bouwman, P. J., Boukamp, B. A., Bouwmeester, H. J. M., Wondergem, H. J. and Notten, P. H. L., "Structural analysis of submicrometer  $\text{LiCoO}_2$  films," *J. Electrochem. Soc.*, **148**, A311 (2001).

Fragnaud, P., Brousse, T. and Schleich, D. M., "Characterization of sprayed and sputter deposited  $\text{LiCoO}_2$  thin films for rechargeable microbatteries," *J. Power Sources*, **63**, 187 (1996).

Lee, L. K., Lee, S. J., Baik, H. K., Lee, H. Y., Jang, S. W. and Lee, S. M., "Substrate effect on the microstructure and electrochemical properties in the deposition of a thin film  $\text{LiCoO}_2$  electrode," *Electrochem. Solid-state Lett.*, **2**, 512 (1999).

Lee, S. J., Lee, J. K., Kim, D. W. and Baik, H. K., "Fabrication of thin film  $\text{LiCo}_{0.5}\text{Ni}_{0.5}\text{O}_2$  cathode for Li rechargeable microbattery," *J. Electrochem. Soc.*, **143**, L268 (1996).

Polo da Fonseca, C. N., Davalos, J., Kleinke, M., Frantini, M. C. A. and Gorenstein, A., "Studies of  $\text{LiCoO}_2$  thin film cathodes produced by r.f. sputtering," *J. Power Sources*, **81-82**, 575 (1999).

Rossen, E., Reimers, J. N. and Dahn, J. R., "Synthesis and electrochemistry of spinel LT- $\text{LiCoO}_2$ ," *Solid State Ionics*, **62**, 53 (1993).

Song, S. W., Han, K. S. and Yoshimura, M., "Effect of 20-200°C fabrication temperature on microstructure of hydrothermally prepared  $\text{LiCoO}_2$  films," *J. Am. Ceram. Soc.*, **83**, 2839 (2000).

Striebel, K. A., Deng, C. Z., Wen, S. J. and Cairns, E. J., "Electrochemical behavior of  $\text{LiMn}_2\text{O}_4$  and  $\text{LiCoO}_2$  thin films produced with pulsed laser deposition," *J. Electrochem. Soc.*, **143**, 1821 (1996).

Wang, B., Bates, J. B., Hart, F. X., Sales, B. C., Zuh, R. A. and Robertson, J. D., "Characterization of thin-film rechargeable lithium batteries with lithium cobalt oxide cathodes," *J. Electrochem. Soc.*, **143**, 3203 (1996).

Whitacre, J. F., West, W. C. and Ratnakumar, B. V., "The influence of target history and deposition geometry on RF magnetron sputtered  $\text{LiCoO}_2$  thin films," *J. Power Sources*, **103**, 134 (2001).

Whitacre, J. F., West, W. C., Brandon, E. and Ratnakumar, B. V., "Crytallographically oriented thin-film nanocrystalline cathode layers prepared without exceeding 300 °C," *J. Electrochem. Soc.*, **148**, A1078 (2001).

Yan, H., Huang, X., Li, H. and Chen, L., "Electrochemical study on  $\text{LiCoO}_2$  synthesized by microwave energy," *Solid State Ionics*, **113-115**, 11 (1998).